SPECIAL PROJECT PROGRESS REPORT

All the following mandatory information needs to be provided. The length should *reflect the complexity and duration* of the project.

Reporting year	2025
Project Title:	Gravity Waves and Turbulence in the Free Atmosphere and the Atmospheric Boundary Layer
Computer Project Account:	SPDESCAN
Principal Investigator:	Dr. Andreas Dörnbrack
Affiliation:	DLR Oberpfaffenhofen Institut für Physik der Atmosphäre Münchener Str. 20 **D – 82230 WESSLING** Germany
Name of ECMWF scientist(s) collaborating to the project (if applicable)	Dr. Christian Kühnlein Dr. Inna Polichtchouk Dr. Nils Wedi Dr. Peter Bechtold
Start date of the project:	2024
Expected end date:	2026

Computer resources allocated/used for the current year and the previous one

(if applicable)
Please answer for all project resources

		Previous year		Current year	
		Allocated	Used	Allocated	Used
High Performance Computing Facility	(units)	500000	110000	500000	8000
Data storage capacity	(Gbytes)	80	80	80	80

Summary of project objectives (10 lines max)

This special project aims at combining high-resolution ground-based and airborne observations with IFS operational forecasts and analyses, with reanalyses, and with results from numerical modelling. The base of our measurements are airborne in-situ observations of the atmospheric wind and temperature in the upper troposphere and lower stratosphere as well as ground-based and airborne remote-sensing observations of temperature in the middle atmosphere. The goal is to analyse the properties of internal gravity waves and of turbulence in the stably stratified atmospheric airflow. A new aspect of our research will be the numerical simulation of the stably stratified atmospheric boundary layer where similar turbulent bursts are observed as in the free atmosphere. The challenge for numerical modelling is to achieve the needed high spatial and temporal resolutions. Furthermore, in this project we want to address the transition to modern computer architectures by applying the newly developed FVM of ECMWF to selected problems.

Summary of problems encountered (10 lines max)

No problems encountered

Summary of plans for the continuation of the project (10 lines max)

This project will be continued as planned.

List of publications/reports from the project with complete references

1. Kaifler, B., N. Kaifler, M. Rapp, and A. Dörnbrack, 2025: Mountain wave momentum flux estimates from airborne lidar measurements in the middle atmosphere above the Southern Andes. *Journal of Geophysical Research: Atmospheres*, under review

2. Wing, R., I. Strelnikova, A. Dörnbrack, M. Gerding, E. Franco-Diaz, L. Holt, M. Mossad, and G.Baumgarten, 2025: Direct Observation of Quasi-monochromatic Gravity Wave Packets Associated with the Polar Night Jet using a Doppler-Rayleigh lidar. *Journal of Geophysical Research: Atmospheres*, accepted 27 June 2025

3. Dörnbrack, A., Lachnitt, H.-C., Hoor, P., & Imazio, P. R., 2025: Multiscale dynamical processes shaping a mixing line. *Journal of Geophysical Research: Atmospheres*, 130, e2025JD043527. https://doi.org/10.1029/2025JD043527

4. Gisinger, S., Bramberger, M., Dörnbrack, A., & Bechtold, P., 2024: Severe convectively induced turbulence hitting a passenger aircraft and its forecast by the ECMWF IFS model. *Geophysical Research Letters*, **51**, e2024GL113037. https://doi.org/10.1029/2024GL113037

5. Dörnbrack, A., 2024: Transient Tropopause Waves, *Journal of the Atmospheric Sciences*, **81**, 1647–1668, https://doi.org/10.1175/JAS-D-24-0037.1

6. Binder, M., & Dörnbrack, A., 2024: Observing gravity waves generated by moving sources with ground-based Rayleigh lidars. *Journal of Geophysical Research: Atmospheres*, 129, e2023JD040156. https://doi.org/10.1029/2023JD040156

7. Achatz, U., J. M. Alexander, E. Becker, H.-Y. Chun, A. Dörnbrack, L. Holt, R. Plougonven, I. Polichtchouk, K. Sato, A. Sheshadri, C. C. Stephan, A. van Niekerk, and C. J. Wright, 2024: Atmospheric Gravity Waves: Processes and Parameterization, *Journal of the Atmospheric Sciences,* **81**, 237–262, https://doi.org/10.1175/JAS-D-23-0210.1

8. Gupta, A., R. Reichert, A. Dörnbrack, H. Garny, R. Eichinger, I. Polichtchouk, B. Kaifler, and T. Birner, 2024: Estimates of Southern Hemispheric Gravity Wave Momentum Fluxes across Observations, Reanalyses, and Kilometer-Scale Numerical Weather Prediction Model. *J. Atmos. Sci.*, **81**, 583–604, https://doi.org/10.1175/JAS-D-23-0095.1.

Summary of selected results

(1) Severe Convectively Induced Turbulence Hitting a Passenger Aircraft and Its Forecast by the ECMWF IFS Model (Gisinger, Bramberger, Dörnbrack, Bechtold, GRL 2024)

Atmospheric turbulence poses a major risk to aviation. Besides airframe damage, it can cause injuries of passengers and crew when encountered unexpectedly. The Singapore Airlines flight SQ321 was on its way from London to Singapore when severe turbulence was encountered over Myanmar on 21 May 2024, see Figure 1. In this paper, it is analysed how well the turbulence was predicted by the computed turbulent eddy dissipation rate (EDR) forecast index of the ECMWF integrated forecasting system (IFS). It was found that ECMWF IFS was able to predict the convection and associated turbulence 24 h in advance. The state-of-the-art probabilistic EDR forecasts based on IFS ensemble members predicted probabilities for EDR > 0.18 $m^{2/3}$ s^{-1} between 10% and 40% over Myanmar with higher values for shorter lead time (8 h forecast). Individual members predicted EDR > 0.18 $m^{2/3}$ s^{-1}. Knowledge about the characteristics of convection in the IFS forecasts is required to make proper use of the probabilities determined from the ensemble for such cases.

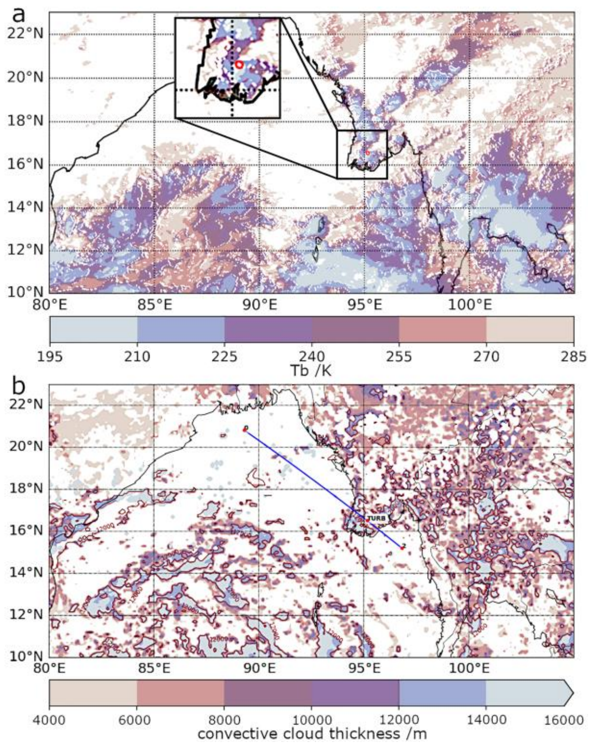

Figure 1: (a) Satellite image of Himawari-8 showing the developing convective clouds by means of brightness temperature (Tb) on 21 May 2024 08 UTC. The red circle shown at location TURB has a diameter of approximately 10 km. The insert shows a zoom to the region of the incident. (b) ECMWF IFS forecast showing the thickness of convective clouds (= height of convective cloud top by parameterized convection minus cloud base height) on 21 May 2024 08 UTC visualized with the MSS tool[1]. Heights of the convective cloud top of 12000 m are marked by the dark red isolines. The forecast was initialized on 20 May 2024 00 UTC.

[1] Rautenhaus, M., Bauer, G., & Dörnbrack, A. (2012). A web service based tool to plan atmospheric research flights. *Geoscientific Model Development*, 5(1), 55–71. https://doi.org/10.5194/gmd-5-55-2012

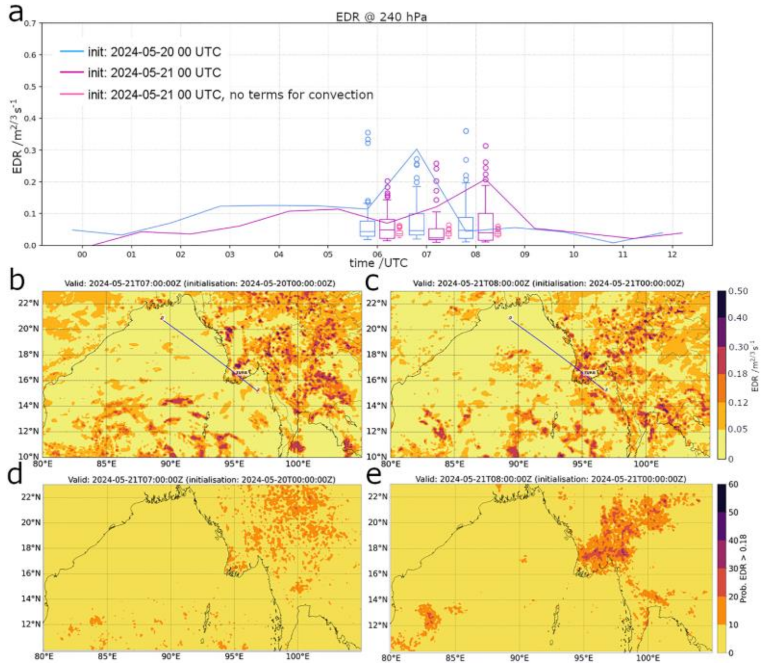

Figure 2: (a) Time series showing EDR at 240 hPa at the location of the incident (TURB) for the IFS HRES forecasts initialized on 20 May 2024 00 UTC with lead time 24–36 hr (blue) and initialized on 21 May 2024 00 UTC with lead time 0–12 hr (purple). Boxplot shows the corresponding IFS ENS (median, 10th/90th percentiles, and maximum extremes) for 06, 07, and 08 UTC including (blue, purple) and without terms for convection (pink) in computing the EDR in the IFS turbulence predictors. (b) EDR ($m^{2/3}$ s^{-1}) at 240 hPa on 21 May 2024 07 UTC of the ECMWF IFS HRES forecast initialized on 20 May 2024 00 UTC (lead time 31 hr) and (c) on 21 May 2024 08 UTC of the ECMWF IFS HRES forecast initialized on 21 May 2024 00 UTC (lead time 8 hr). Maps were visualized with the MSS tool (d), (e) Corresponding probability for EDR > 0.18 $m^{2/3}$ s^{-1} computed from the IFS ENS.

IFS forecasts initialized on 00 UTC each day are available after computation at around 9 UTC the same day. Figure 2 shows the 12 h time series of the IFS EDR forecast at 240 hPa at the location of the turbulence encounter (TURB) of flight SQ321, which departed from London on 20 May 2024 at 21:38 UTC. The IFS forecast initialized on 20 May 2024 00 UTC is the latest forecast available prior to departure, so it could have been used by the airline.

The HRES forecast initialized on 20 May 00 UTC shows a maximum in EDR = 0.30 $m^{2/3}$ s^{-1} at 7 UTC followed by low values less than 0.1 $m^{2/3}$ s^{-1} afterward until 12 UTC which is 21:30 local time in Myanmar. The HRES values lie at the upper edge when compared to the other 50 IFS ENS ensemble members at 6 UTC and 7 UTC and close to the median at 8 UTC. The IFS ENS shows an increase of the 90th percentile from about 0.12 $m^{2/3}$ s^{-1} at 6 UTC to about 0.2 $m^{2/3}$ s^{-1} at 8 UTC while the median remains well below 0.1 $m^{2/3}$ s^{-1}.

The HRES forecast initialized a day later on 21 May 00 UTC shows a maximum in EDR of 0.2 $m^{2/3}$ s^{-1} at 8 UTC which is close to the 90th percentile of the ENS. However, individual members show values well above 0.2 $m^{2/3}$ s^{-1} at 7 UTC and 8 UTC just in between the time when the turbulence encounter of flight SQ321 happened at 7:49 UTC. Additional sensitivity runs with the IFS ENS show a narrow distribution with EDR close to 0.05 $m^{2/3}$ s^{-1} when only contributions by the vertical diffusion scheme are considered and the terms for convection are omitted.

The probability for EDR > 0.18 $m^{2/3}$ s^{-1} determined from the ENS members of the forecast initialized on 20 May 2024 00 UTC is 12% for 8 UTC at 240 hPa at TURB. When the ENS EDR maxima of ± 2 grid points from TURB (± 0.2° in latitude and longitude, respectively) are considered, which incorporates the uncertainty of the location of convection among the ENS members, the probability for EDR increases to 36%.

Horizontal maps of EDR at 240 hPa for both HRES forecasts are shown for the time of maximum EDR at TURB, that is 7 UTC for initialization on 20 May 00 UTC (Figure 2b) and 8 UTC for the initialization on 21 May 00 UTC (Figure 2c). Enhanced EDR is mainly found over land and in the ITCZ which corresponds to the occurrence of convection (Section 2.2). It is the convective momentum transport that dominated the IFS EDR forecast that day. Both HRES forecasts agree as such that they show the highest risk to encounter severe turbulence along the flight track over Myanmar (Figures 2b and 2c) near the location of the turbulence encounter of flight SQ321. Horizontal maps of the ENS probability for EDR > 0.18 $m^{2/3} s^{-1}$ (Figures 2d and 2e) reveal probabilities of 10%–20% over land associated with the predicted occurrence of convection. Local probabilities of 30%–40% were found for shorter lead time (initialized on 21 May 2024 00 UTC, lead time 8 h) and the area with enhanced probabilities becomes more focused in a band-like pattern (Figure 2e) which compares well with the convection in the satellite image (Figure 1a).

The results presented in this study show that the turbulence forecasts available from ECMWF provide valuable information on convection and CIT, as encountered by flight SQ321, along route prior to departure. As such the forecast could have helped to make the crew aware of potential occurrence of turbulence by convection in the area and to take precautions like switching on the fasten seat belt sign, postponing board service, and request updates by nowcasting services. The implementation of a probabilistic turbulence forecast based on the IFS ensemble was essential. However, training is required in order to learn the characteristics of the IFS forecasts for convection and to make proper use of the ENS probabilities for moderate and severe turbulence.

The paper discusses multiscale dynamical processes shaping a mixing line in the upper troposphere/lower stratosphere (UTLS). It focuses on aircraft observations above southern Scandinavia during a mountain wave event and how they can be analysed based on dynamic variables and the trace gases N_2O and CO. This study aims to identify the irreversible component of the stratosphere-troposphere exchange.

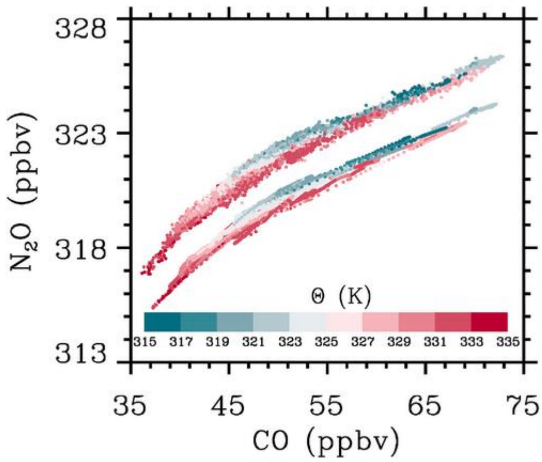

Figure 3: N_2O-CO relation of in situ airborne measurements along the flight tracks RF07FL2 and RF08FL1. The upper group of data points refers to the 1 Hz data. The lower data group is offset vertically by $\Delta N_2O = -2$ ppbv and shows the same data but smoothed by a boxcar average of 80 s length, that is, of ~20 km wavelength. The colour shading indicates the potential temperature Θ.

It was shown that the overall shape of the mixing line in Figure 3 is determined by the large-scale and mesoscale atmospheric conditions in the UTLS. Especially, the wide range of values along the flight tracks causes a compact, almost linear tracer-tracer relation between N_2O and CO. Only motion components with scales less than 4 km lead to the observed scatter around the mixing line, see the smoothed tracer-tracer relation in Figure 3. The anisotropic and patchy nature of the observed turbulence is responsible for this scatter in N_2O and CO. The turbulence analysis reveals different scaling laws for the power spectra upstream, over the ridge and downstream of the mountains that lead to energy dissipation and irreversible mixing. The study suggests that turbulence dynamics may follow a cycle starting with 3D homogeneous isotropic turbulence upstream, transitioning to anisotropic turbulence over the ridge and further downstream. This transition is attributed to an interplay between turbulent eddies and internal gravity waves.